Journal of Alzheimer's Disease 75 (2020) 531–545
DOI 10.3233/JAD-191175
IOS Press

Identification of Novel Genes Associated with Cortical Thickness in Alzheimer's Disease: Systems Biology Approach to Neuroimaging Endophenotype

Bo-Hyun Kim[a], Yong-Ho Choi[a], Jin-Ju Yang[a], SangYun Kim[b], Kwangsik Nho[c,*] and Jong-Min Lee[a,*] for the Alzheimer's Disease Neuroimaging Initiative[1]
[a]*Department of Biomedical Engineering, Hanyang University, Seoul, Korea*
[b]*Department of Neurology, Seoul National University College of Medicine and Clinical Neuroscience Center of Seoul National University Bundang Hospital, Seongnam, Korea*
[c]*Department of Radiology and Imaging Sciences, Indiana Alzheimer Disease Center, Indiana University School of Medicine, Indianapolis, IN, USA*

Handling Associate Editor: Keeley Brookes

Accepted 6 March 2020

Abstract. Alzheimer's disease (AD) is a common neurodegenerative disorder characterized by a heterogeneous distribution of pathological changes in the brain. Cortical thickness is one of the most sensitive imaging biomarkers for AD representing structural atrophy. The purpose of this study is to identify novel genes associated with cortical thickness. We measured the whole-brain mean cortical thickness from magnetic resonance imaging (MRI) scans in 919 subjects from the Alzheimer's Disease Neuroimaging Initiative cohort, including 163 AD patients, 488 mild cognitive impairment patients, and 268 cognitively normal participants. Based on the single-nucleotide polymorphism (SNP)-based genome-wide association study, we performed gene-based association analysis for mean cortical thickness. Furthermore, we performed expression quantitative trait loci, protein-protein interaction network, and pathway analysis to identify biologically functional information. We identified four genes (*B4GALNT1*, *RAB44*, *LOC101927583*, and *SLC26A10*), two pathways (cyclin-dependent protein kinase holoenzyme complex and nuclear cyclin-dependent protein kinase holoenzyme complex), and one protein-protein interaction (B4GALNT1 and GALNT8 pair). These genes are involved in protein degradation, GTPase activity, neuronal loss, and apoptosis. The identified pathways are involved in the cellular processes and neuronal differentiation, which contribute to neuronal loss that is responsible for AD. Furthermore, the most significant SNP (rs12320537) in *B4GALNT1* is associated with expression levels of *B4GALNT1* in several brain regions. Thus, the identified genes and pathways provide deeper mechanistic insight into the molecular basis of brain atrophy in AD.

Keywords: Alzheimer's disease, brain, cortical thickness, gene-based association analysis, genome-wide association study, imaging genetics

*Correspondence to: Jong-Min Lee, PhD, Department of Biomedical Engineering, Hanyang University, Sanhakgisulkwan #319, Wangsimni-ro Seongdong-gu, Seoul, 04763, Korea. Tel.: +82 2 2220 0685; E-mail: ljm@hanyang.ac.kr. and Kwangsik Nho, PhD, Department of Radiology and Imaging Sciences, Indiana Alzheimer Disease Center, Indiana University School of Medicine, Indianapolis, IN 46202, USA. Tel.: +1 317 963 7503; E-mail: knho@iupui.edu.

[1]Data used in preparation of this article were obtained from the Alzheimer's Disease Neuroimaging Initiative (ADNI) database (http://adni.loni.usc.edu). As such, the investigators within the ADNI contributed to the design and implementation of ADNI and/or provided data but did not participate in analysis or writing of this report. A complete listing of ADNI investigators can be found at: http://adni.loni.usc.edu/wp-content/uploads/how_to_apply/ADNI_Acknowledgement_List.pdf

INTRODUCTION

Alzheimer's disease (AD) is a common neurodegenerative disorder characterized by progressive loss of cognitive functions and memory caused by neuronal dysfunction and death [1]. The heritability of AD is reported as 60%–80% [2], and *APOE ε4* is well known as one of the major genetic factors that increases the risk for AD [3, 4]. Large-scale genome-wide association studies (GWAS) identified more than 20 genes as potential susceptibility genes in AD, including *BIN1*, *CLU*, and *CR1* [5–7]. However, all known AD susceptibility genes, including *APOE*, explain only a small portion of the genomic variance of AD [8, 9], referred to as the "missing heritability". One of the suggested explanations for this problem is the phenotypic heterogeneity [8–13].

Traditional case-control GWAS for psychiatric and neurodegenerative disorders exhibit classification and long-term stability issues, because their definition and diagnosis are based on behavioral characteristics and cognitive deficits that are generally difficult to quantify [13, 14]. Clinical heterogeneity is increasingly recognized as a common characteristic of AD. Machia et al. found that clinical heterogeneity (also called phenotypic heterogeneity) reduced statistical power of the conducted analyses [15]. The endophenotype conceptual analysis has been proposed to improve the power of association studies by reducing phenotypic heterogeneity [16]. The endophenotype is a measurable component (i.e., by neurological, neuroanatomical, cognitive, and neuropsychological data), which lies along the pathway between the genotype and the disease [17–20].

Imaging genetics is an integrated research field that assesses the impact of genetic variation on neuroimaging measures, which has been applied in various diseases including AD [21–25]. Brain structural atrophy has been proposed as a marker of AD progress [26, 27], and subcortical atrophy measurements such as the hippocampal volume and intracranial volume (ICV) were used as endophenotypes in previous imaging genomic studies [22, 28, 29]. Cortical thickness is one of the most sensitive imaging biomarkers for disease-related brain atrophy. Whole-brain mean cortical thickness and regional mean cortical thickness (inferior frontal, medial temporal, anterior and posterior cingulate, lateral occipital regions, etc.) have been widely studied to demonstrate their abnormal reduction in patients with AD compared with cognitively normal control subjects [30–34]. The heritability of cortical thickness is reported as 69% [35], and identified genetic variants from previous studies that are associated with cortical thickness [23, 36, 37], accounted for a small portion of the variance. Correspondingly, more susceptibility genes need to be identified to explain the missing heritability of cortical thickness.

GWAS with single-nucleotide polymorphism (SNP) are an important step. However, SNP-based analysis applies a strict level of significance (typically 5×10^{-8}) to control type-1 errors, thus, SNPs that have modest effects could be ignored [38, 39]. Gene-based analysis considers the gene as a basic unit for association analysis, and it can address this problem by combining the *p*-values from all SNPs in a gene to increase the statistical power [39–41]. This method has been employed as a complementary technique for SNP-based GWAS to identify disease susceptibility genes [42]. Furthermore, integrating gene-based analysis with biological information, such as protein-protein interaction (PPI) and pathways, contributes further to the understanding of the association between genetic variation and disease [38, 43, 44]. The network analysis using PPI information can elucidate gene–gene interactions and identify susceptibility genes that are weakly associated with the disease [39]. The pathway analysis that considers the gene set as a unit of analysis could provide valuable insight to the understanding of the biological process of the disease [45].

The purpose of this study is to identify novel susceptibility genes that contribute to cortical thickness. In this study, we performed gene-based GWAS with cortical thickness in patients with AD. The advantage of using cortical thickness as an endophenotype is that it represents a relatively simpler clue to genetic underpinnings than the disease diagnosis [17]. The endophenotype lies along the pathway between genotype and phenotype, and the causal relationship between the endophenotype and phenotype are at times bidirectional [46]. Therefore, to isolate the genetic effect component that cannot be attributed to the disease-status difference, we applied the disease status as a covariate for this study [47]. We performed gene-based analysis, PPI network and pathway analysis with mean cortical thickness and performed eQTL to understand the functional roles of genetic variants.

Table 1
Demographic information for 919 ADNI participants

	ADNI-1 ($n = 592$)	ADNI-GO/2 ($n = 327$)
Age (y) (mean ± s.d.)	75.59 ± 6.56	72.99 ± 7.18
Sex (male/female)	358 / 234	183 / 144
Education (y) (mean ± s.d.)	15.67 ± 3.00	16.16 ± 2.66
Diagnosis (AD/MCI/CN)	139 / 286 / 167	24 / 202 / 101
APOE ε4 (0/1/2 copies)	295 / 231 /66	194 / 109 /24

AD, Alzheimer's disease; MCI, mild cognitive impairment; CN, cognitively normal controls; *APOE* ε4 represents the number of ε4 copies in rs429358 and rs7412 single nucleotide polymorphism (SNP)

MATERIALS AND METHODS

Subjects

Neuroimaging and genetic data were acquired from 940 subjects as part of the Alzheimer's Disease Neuroimaging Initiative (ADNI), including AD, mild cognitive impairment (MCI), and cognitively normal controls (CN) [48–50]. Magnetic resonance (MR) image processing failed for 21 subjects, which were consequently excluded from all analyses. The final sample included 163 AD, 488 MCI, and 268 CN subjects from ADNI–1 and ADNI-GO/2 (total N = 919). The demographic and genotypic characteristics of the subjects are listed in Table 1.

Imaging acquisition and processing

Three-dimensional T1-weighted baseline brain MR images were acquired from ADNI, as previously described [48]. All T1-weighted MRIs were processed using automatic image analysis pipeline software (CIVET) developed by the Montreal Neurological Institute. MR images acquired from all the subjects were corrected for non-uniform intensity and normalized to a standard space using linear transforms [51, 52]. The registered MR images were classified into gray matter (GM), white matter (WM), and cerebrospinal fluid, using an advance neural net classifier [53]. The hemispherical WM and GM surfaces, consisting of 40,962 vertices, were extracted using the constrained Laplacian-based automated segmentation with proximities (CLASP) algorithm [54, 55]. Finally, the cortical thickness was calculated as the Euclidean distance between the corresponding vertices of the GM and WM surfaces [56]. The mean cortical thickness was calculated as the average of cortical thicknesses of all 81,924 vertices.

Genotyping and quality control

The GWAS genotype data were downloaded from the ADNI website (http://www.loni.ucla.edu/ADNI). Genotyping was performed using the Illumina Human610–Quad BeadChip in ADNI–1 and the Illumina HumanOmniExpress BeadChip in ADNI-GO/2 [57, 58]. Since the Illumina chip did not include the SNPs associated with *APOE* alleles, we downloaded the genotype data of two *APOE* SNPs (rs429358, and rs7412) that define the epsilon 2, 3, and 4 alleles from the ADNI website (http://www.loni.ucla.edu/ADNI). Each dataset from ADNI-1 and ADNIGO/2 was independently imputed using IMPUTE2 [59] with the 1000 Genome Project phase 1 samples as a reference panel [60]. The quality control was performed using PLINK v1.9 software (http://zzz.bwh.harvard.edu/plink/) [61], whereby the individual markers were removed from the analyses that did not satisfy the following criteria: genotype call rate < 95%, HWE $p < 10^{-6}$ (in controls), and MAF < 5%. Finally, 3,041,429 bi-allelic SNPs in autosomal chromosomes (i.e., sex chromosomes, mitochondrial, and pseudo-autosomal SNPs were excluded). In order to prevent spurious association due to population stratification [62], we selected only non-Hispanic participants of European ancestry that clustered with CEU (Utah residents with Northern and Western European ancestry from the CEPH collection) or TSI (Toscani in Italia) populations in the HapMap genotype data using multidimensional scaling analysis (MDS).

Statistical analysis

Gene-based association analysis

Gene-based association analysis calculates gene-based *p*-values by combining SNP-based *p*-values from GWAS. SNP-based *p*-values were calculated using a linear regression with the additive model using PLINK. We used age, sex, education, disease diagnosis, scanner field strength, APOE4 genotype as covariates, whereas the intracranial volume (ICV) was not used because the cortical thickness is known to be not correlated with ICV [36, 63–65]. Gene-based association analysis was performed using the gene-based association test using extended Simes procedure (GATES), which applies the extended Simes procedure to calculate a summary *p*-value for each gene [38]. The linkage disequilibrium (LD) was calculated using 1000 Genomes Project European samples [60]. SNPs whose $r^2 < 0.005$ were ignored

in the next gene annotation step, and SNPs that fell within 5 kb of the 3'/5' untranslated regions were considered "within" the genes on the human genome (hg19) coordinates. A total of 3,041,429 SNPs and their *p*-values from GWAS were used for gene-based analyses, where SNPs were annotated into 24,190 autosomal genes, and their corresponding *p*-values were calculated. To correct for multiple hypothesis testing, we employed the false discovery rate (FDR) method [66], and genes with FDR-corrected *p*-values < 0.05 were considered significant. Following the GWAS, *post hoc* models including age, sex, education, scanner field strength, and APOE4 genotype as covariates were used to assess the genetic effects on phenotype in each diagnosis. These *post hoc* models used peak SNPs mapped to identified genes from gene-based analysis.

Expression quantitative trait loci analysis

To identify the functional effect of genetic variants on the gene expression, we performed expression quantitative trait loci (eQTL) analysis. Gene expression levels and genotype data were downloaded from the Braineac database (http://www.braineac.org/) [67]. We used the expression levels of identified genes from gene-based association analysis and the genotype of most significant SNP in each gene. The expression levels in 10 brain tissues, including the hippocampus, substantia nigra, WM, frontal, temporal, and occipital cortex were downloaded from the Braineac database, and eQTLs with FDR-corrected *p*-values < 0.05 were considered significant.

Vertex-wise association analysis

Vertex-wise ANCOVA analyses were performed with the Surfstat software for Matlab (http://www.math.mcgill.ca/keith/surfstat/). One-way ANOVA analysis was used to assess the effect of rs236490 and rs12320537 genotypes (0, 1, and 2) on vertex-wise cortical thickness. Cortical thickness on 81,81924 vertices was controlled for the same covariates used in SNP-based GWAS. Genotype differences among 0, 1, and 2 were corrected for multiple comparisons (FDR-corrected $p < 0.05$).

Protein-protein interaction network analysis

The protein-protein interaction (PPI) dataset was downloaded from the search tool for the retrieval of interacting genes/proteins (STRING; https://string-db.org/), which is a database of known and predicted interactions, including direct (physical) and indirect (functional) interactions derived from high-throughput experiments, genomic context, mining of literature, and co-expression [68]. High-confidence networks (confidence score > 0.7) consisting of 10,897 proteins (nodes) and 157,061 interactions (edges) were used to minimize type-1 errors. The confidence scores indicated the estimated likelihood that a given interaction was biologically meaningful, specific, and reproducible, given the supporting evidence [68]. We performed PPI network analysis using the HYbrid Set-based Test (HYST) tool, which combined gene-based *p*-values for each protein interaction and detected PPI pairs, where two genes are associated with the phenotype [69]. For each protein-protein interaction pair, the first gene-based *p*-values were calculated using GATES, and the scaled chi-square test was then performed to combine gene-based *p*-values into a single test statistic with corrections for the LD between genes. The Higgins I^2, which is mostly applied to detect the heterogeneity in meta-analysis, was used to identify PPI pairs, whereby both genes were potentially associated with the phenotype [70]. PPI pairs with Higgins $I^2 > 0.5$ were excluded, which implies that only one gene in a PPI pair is associated with the phenotype. PPI pairs with FDR-corrected *p*-values < 0.05 were considered significant.

Pathway analysis

Pathway analysis was performed to identify functional gene sets associated with the phenotype. The GO (http://geneontology.org) database was used to define gene sets representing biological pathways. The biological significance of gene sets was evaluated using the HYST tool [69] with restricted pathways containing 5 to 200 genes to limit the potential for possible size-influenced associations [45, 70]. In total, 5,128 gene sets were tested in a pathway analysis, where the genome-wide significance threshold for gene sets was 1.39×10^{-5} according to the FDR correction method.

RESULTS

Gene-based association analysis

Before the gene-based association analysis, we performed SNP-based GWAS with mean cortical thickness. The mean cortical thickness is normally distributed (Supplementary Figure 1) and there were significant group differences in mean cortical thickness across three diagnosis groups (Supplementary Figure 2, $p = 1.13 \times 10^{-21}$). No marker passed the

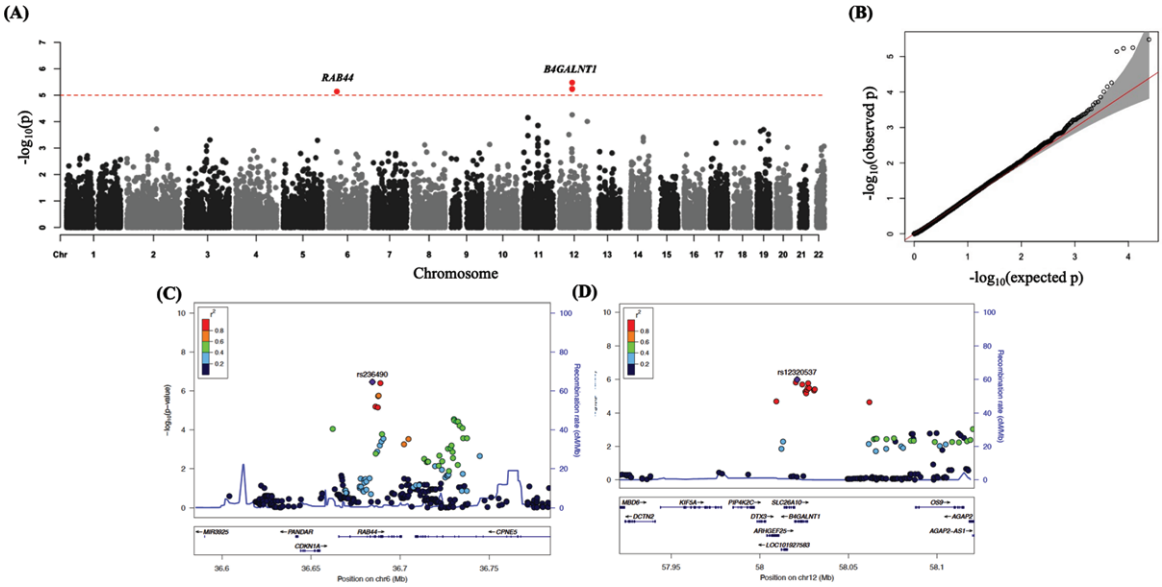

Fig. 1. **Gene-based and SNP-based GWAS results for cortical thickness**. (A) Manhattan plot of gene-based *p*-values. The horizontal axis (x-axis) shows the start position of each gene on the autosomal chromosome, and the vertical axis (y-axis) shows the observed gene-based $-\log_{10}(p)$ for the association. Red horizontal lines indicate a genome-wide significant threshold ($p < 1 \times 10^{-5}$, which approximately corresponds to a threshold of the FDR-corrected $p < 0.05$). (B) Quantile-Quantile (Q-Q) plot of gene-based *p*-values. Observed $-\log_{10}(p)$ (y-axis) were plotted against those expected under the null hypothesis (x-axis). C, D) Regional association plot of SNP-based GWAS *p*-values. All SNPs within 100 kb of the *RAB44* gene on chromosome 6 (C) and the *B4GALNT1* gene on chromosome 12 (D) are plotted based on their GWAS $-\log_{10}(p)$, NCBI human genome build 37, and recombination rates calculated from the 1000 Genomes Project reference data. The most significant SNP is highlighted in violet. The color scale of r^2 values is used to label SNPs based on their degree of LD with rs236490 and rs12320537, respectively. Genes in the region are labeled with arrows denoting the 5'–3' orientation. All plots were adapted from LocusZoom results.

genome-wide significance threshold of 5×10^{-8} in SNP-based GWAS (Supplementary Figure 3). In the gene-based association analysis, 1,702,233 SNPs (53.31%) were mapped to 24,190 genes on the human genome. The gene-based association analysis revealed that four genes (*B4GALNT1*, *LOC101927583*, *SLC26A10*, *RAB44*) were significantly associated with the mean cortical thickness (Fig. 1, Supplementary Table 1). The *B4GALNT1* gene was found to be most significantly associated with cortical thickness ($p = 3.34 \times 10^{-6}$, corrected $p = 0.044$). Two additional genes, *LOC101927583* and *SLC26A10* adjacent to the B4GALNT1 gene on chromosome 12, also yielded significant associations ($p = 5.69 \times 10^{-6}$, corrected $p = 0.044$; $p = 5.95 \times 10^{-6}$, corrected $p = 0.044$, respectively). Furthermore, the *RAB44* gene on chromosome 6 also exhibited a significant association ($p = 7.29 \times 10^{-6}$, corrected $p = 0.044$). The most significant SNPs in *RAB44* and *B4GALNT1* genes from SNP-based GWAS were rs236490 and rs12320537 (Fig. 1, Supplementary Table 2). These two SNPs showed a protective effect on brain structural atrophy, i.e., participants with minor alleles have larger cortical thickness compared to those without minor alleles (Supplementary Table 1, Supplementary Figure 4). In *post hoc* analysis, the association trends of rs236490 with mean cortical thickness in each diagnosis group were similar, i.e., participants with at least one minor allele have larger cortical thickness compared to participants without minor alleles. For rs12320537, participants with at least one minor allele have larger cortical thickness, especially in MCI group (Supplementary Figure 5). Other peak SNPs are highly correlated with rs236490 and rs12320537, respectively.

Expression quantitative trait loci (eQTL) analysis

To identify the functional effect of genetic variants on the gene expression, we performed the eQTL analysis. As the gene expression of *LOC101927583* was not present in the Braineac database, we leveraged three identified genes (*RAB44*, *SLC26A10*, *B4GALNT1*) from gene-based association analysis and their peak SNPs (rs236490 and rs12320537).

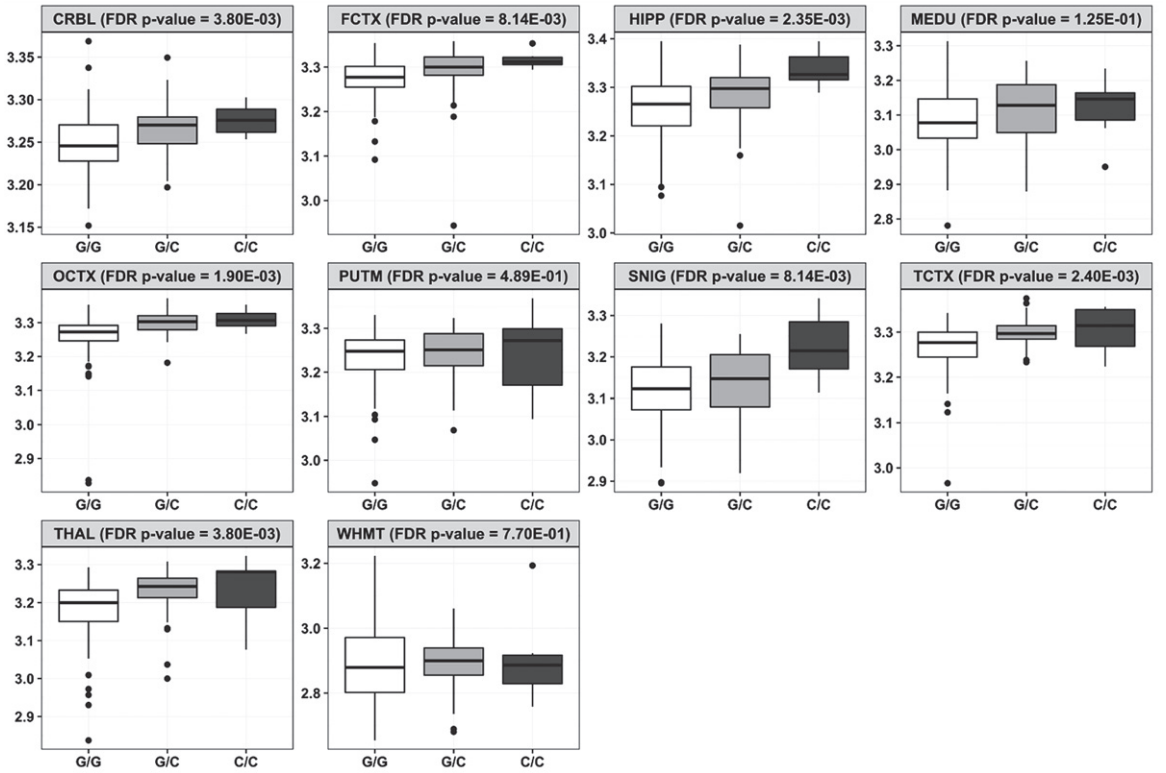

Fig. 2. **Effect of rs12320537 on *B4GALNT1* expression level**. Expression quantitative trait loci (eQTL) box plots of association between genotypes of rs12320537 with expression levels of *B4GALNT1* in ten brain regions. The y-axis represents expression levels of *B4GALNT1*. CRBL, cerebellar cortex; FCTX, frontal cortex; HIPP, hippocampus; MEDU, medulla; OCTX, occipital cortex; PUTM, putamen; SNIG, substantia nigra; TCTX, temporal cortex; THAL, thalamus; WHMT, intralobular WM.

We found that rs12320537 in *B4GALNT1* significantly regulated the expression of *B4GALNT1* in several brain regions, including the temporal cortex (FDR-corrected $p = 2.40 \times 10^{-3}$) and hippocampus (FDR-corrected $p = 2.35 \times 10^{-3}$), which are the AD-related brain regions (Fig. 2). rs12320537 and rs236490 did not exhibit any significant correlation with expression levels of *SLC26A10* and *RAB44*, respectively, after multiple comparison corrections.

Vertex-wise association analysis

We performed the one-way ANCOVA analysis to assess the effect of two SNPs (rs236490 and rs12320537) on vertex-wise cortical thickness. rs236490 showed significant associations in bilateral frontal, parietal, and temporal lobes (Fig. 3A). Significant effects of rs12320537 were observed in the left frontal and bilateral temporal lobes (Fig. 3B). These two SNPs showed significant effects on cortical thickness of AD-related brain regions, including the left inferior frontal gyrus, parahippocampal gyrus, inferior, and superior temporal gyrus.

Protein-protein interaction network analysis

We tested 157,050 gene pairs consisting of 24,190 genes to identify AD susceptibility genes associated with the mean cortical thickness by combining statistical genetic results and physical interaction information of their respective gene products. Protein-protein interaction (PPI) pairs with a $p < 2.27 \times 10^{-7}$ were considered as significant according to the FDR correction. One PPI pair with $I^2 < 0.5$ yielded a significant association (Table 2). The PPI pair involving B4GALNT1 and GALNT8 (polypeptide N-acetylgalactosaminyltransferase 8) on chromosome 12 exhibited significant association ($p = 2.27 \times 10^{-7}$). The *B4GALNT1* gene was significantly associated with the cortical thickness in gene-based association analyses ($p = 3.34 \times 10^{-6}$, corrected $p = 0.044$), however the *GALNT8* gene did

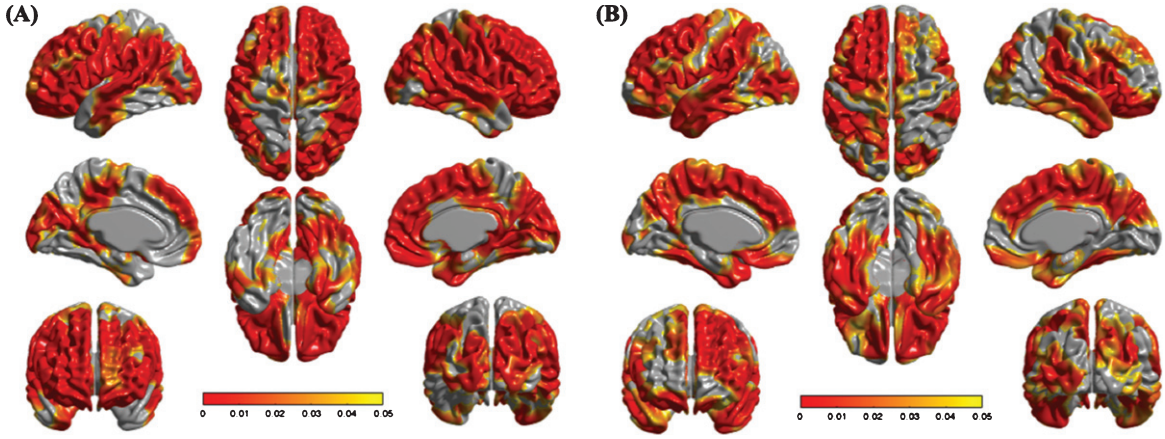

Fig. 3. **Effect of rs236490 and rs12320537 on vertex-wise cortical thickness**. Effect of genotypes (0, 1, or 2) on cortical thickness. The color scale indicates statistical p-maps corrected for multiple comparisons (FDR-corrected $p < 0.05$). Significant effects of rs236490 on cortical thickness were observed in widespread bilateral frontal, parietal, temporal lobes and the right parahippocampal gyrus (A). Most significant effects of rs12320537 were observed in the left frontal and bilateral temporal lobes (B).

Table 2
Peak PPI pairs ($I^2 < 0.5$) associated with mean cortical thickness

Gene1_CHR	Gene1	Gene2_CHR	Gene2	Confidence score	*p*-value for Cochran's Q	I^2	*p*-value
12	**B4GALNT1**	12	**GALNT8**	0.768	0.201	0.389	2.27×10^{-7}
12	ARHGEF25	13	EDNRB	0.914	0.522	0.000	1.46×10^{-6}
19	OR7A10	1	OR14A16	0.899	0.608	0.000	9.54×10^{-6}
11	SF1	22	DDX17	0.988	0.766	0.000	1.33×10^{-5}
12	ARHGEF25	1	PTAFR	0.899	0.215	0.349	1.41×10^{-5}
14	SNW1	9	NOTCH1	0.995	0.704	0.000	1.64×10^{-5}
12	ARHGEF25	5	F2RL2	0.899	0.185	0.430	1.85×10^{-5}
12	ARHGEF25	8	TRHR	0.899	0.159	0.497	2.41×10^{-5}
12	ARHGEF25	17	GAST	0.899	0.144	0.532	2.81×10^{-5}
19	OR7A10	11	OR9Q2	0.899	0.422	0.000	2.88×10^{-5}

Gene1_CHR, chromosome on which the gene1 is located; Gene2_CHR, chromosome on which gene2 is located; I^2, Higgins's I^2; p, PPI-based *p*-value. PPI pair with FDR-corrected *p*-value < 0.05 is indicated in bold in the table.

not reach the genome-wide significance threshold in both the SNP-based GWAS and the gene-based test (GWAS $p = 4.23 \times 10^{-4}$, gene-based $p = 3.53 \times 10^{-3}$).

Pathway-based analysis

We performed a pathway-based association analysis using 5,128 pathways from the GO database to identify biologically significant pathways. We identified two pathways that exhibited higher association to mean cortical thickness (FDR-corrected $p < 0.05$) (Table 3). The most significant pathways were the nuclear-cyclin-dependent protein kinase holoenzyme complex ($p = 1.36 \times 10^{-5}$) and the cyclin-dependent protein kinase holoenzyme complex ($p = 1.39 \times 10^{-5}$). In addition, we identified 28 potential AD susceptibility genes included in these two pathways (Supplementary Table 3). We compared the genes in two identified pathways with AD-related genes from the Phenopedia [72] (https://phgkb.cdc.gov/PHGKB/startPagePhenoPedia.action) database. Among the 28 genes included in the two identified pathways, 5 genes were previously reported to be associated with AD. The *p*-values of these genes were unremarkable in the SNP-based GWAS, gene-based, and PPI network association analyses.

DISCUSSION

This study performed a genetic association study to identify novel genes affecting cortical thickness and found four genes, one PPI pair and two pathways associated with mean cortical thickness. Our eQTL and vertex-wise associations analysis provide

Table 3
Peak pathways associated with mean cortical thickness

Category	GO ID	GO name	Gene set size	*p*-value
CC	**GO:0019908**	**Nuclear cyclin-dependent protein kinase holoenzyme complex**	15	1.36×10^{-5}
CC	**GO:0000307**	**Cyclin-dependent protein kinase holoenzyme complex**	28	1.39×10^{-5}
BP	GO:0086009	Membrane repolarization	14	2.10×10^{-4}
CC	GO:0032806	Carboxy-terminal domain protein kinase complex	20	2.60×10^{-4}
MF	GO:0005112	Notch binding	16	3.70×10^{-4}
BP	GO:0030007	Cellular potassium ion homeostasis	12	4.50×10^{-4}
CC	GO:1902911	Protein kinase complex	78	6.20×10^{-4}
BP	GO:0055075	Potassium ion homeostasis	18	6.30×10^{-4}
BP	GO:0045618	Positive regulation of keratinocyte differentiation	12	6.50×10^{-4}
BP	GO:0032271	Regulation of protein polymerization	156	7.50×10^{-4}

BP, biological process; CC, cellular component; MF, molecular function; GO ID, Gene ontology term ID; Gene Set Size, the number of genes in GO terms. Gene sets with FDR-corrected *p*-value < 0.05 are indicated in bold in the table.

further evidence on identified genes from gene-based association analysis.

Although previous GWAS identified some SNPs associated with cortical thickness [23, 36, 37], identified variants could explain a small proportion of phenotypic variance of cortical thickness. SNP-based GWAS ignored the loci with moderate association signals due to the adoption of a stringent significance threshold. Furthermore, because of the stringent threshold, the reported loci were hard to replicate in other studies. Gene-based association analysis is the complementary approach that combines *p*-values from all SNPs in a gene to augment statistical power. In this gene-based association analysis, we identified four genes associated with cortical thickness. In SNP-based GWAS, no marker passed the genome-wide significance threshold of 5×10^{-8}. However, we confirmed that the most significant SNP in *B4GALNT1* regulates the expression of *B4GALNT1*. Moreover, the most significant SNPs in two genes are significantly associated with the vertex-wise cortical thickness in AD-related brain regions.

One of the most associated genes with cortical thickness in this study is *B4GALNT1*, which is a GM2/GD2 synthase involved in the biosynthesis of complex gangliosides. Gangliosides, glycosphingolipids that contain sialic acid, constitute an important cellular component [73]. The brain includes various gangliosides, which play an important role in maintaining the integrity of the nervous system and neuronal development [74–76]. GM1, one of the major gangliosides in the brain, binds to Aβ to form a GM1-bound Aβ (GAβ), which then leads to the formation of amyloid fibrils in AD brains [77]. Deletion of enzyme encoded by *B4GALNT1* results in a loss of series-a and series-b gangliosides in mouse [78] and human brain [79]. Several earlier studies indicated the alteration of ganglioside metabolism in the AD brain [80–82]. Kraun et al. reported that ganglio-series gangliosides including GM1, GD1a, GD1b, and GT1b were decreased in temporal and frontal cortex in AD brain [82]. The *B4GALNT1* knock out mice showed progressive motor deficits with age [83] and deletion of *B4GALNT1* in human results in severe spastic paraplegia [84]. Although the expression of B4GALNT1 regulates the expression of BACE1 protein (β-site AβPP cleaving enzyme 1) which is the major enzyme for the β-site cleavage of the amyloid-β precursor protein (AβPP) in mice model, it does not mRNA levels [85]. Furthermore, the most prominent SNP in *B4GALNT1*, rs12320537, was significantly associated with the expression levels of *B4GALNT1* in several brain regions of control subjects with normal cognition ($p < 0.05$), especially in the cerebellar cortex, frontal cortex, occipital cortex, temporal cortex, substantia nigra, hippocampus, and thalamus (Braineac database (http://www.braineac.org/)). Thus, *B4GALNT1* may influence not only the formation of amyloid fibrils, but is also associated with neuronal death in the brain cortex.

RAB44 is the component of guanosine-5'-triPhosphate (GTP)-ase activity and GTP binding, where GTP plays an important role in signal transduction and protein biosynthesis. Udayar et al. reported that the silencing of RAB44 decreased Aβ levels. Furthermore, RAB proteins are responsible for regulating the β-cleavage and controlling the levels of Aβ [86]. The RAB family of GTPases was reported to be associated with AD [87–89]. RAB proteins were indicated to be upregulated in hippocampal neurons of individuals with MCI and AD,

and the RAB GTPase expression increased endocytic pathway activity, which may result in long-term deficits in hippocampal neurotrophic signaling, and thus represents a key pathogenic mechanism underlying AD progression [88]. Furthermore, Kawauchi et al. reported that RAB-dependent trafficking pathways are associated with neuronal migration, which is an essential step in the formation of the six-layers of the cerebral cortex [90].

In PPI network analyses, *GALTN8* is a protein-coding gene that is related to carbohydrate binding and voltage-gated potassium channel activity. Herold et al. reported that rs116938548 ($p = 2.00 \times 10^{-7}$), an intergenic SNP mapped to the *GALNT8* gene, was associated with AD [91]. Moreover, two genes (*CD33* and *ASGR2*), that make up components of carbohydrate binding, were previously reported to be associated with AD [92, 93]. Voltage-gated potassium channels are the regulators of neuronal excitability [94], extensively distributed in central and peripheral nervous systems. They promote neuronal apoptosis [95], thus contributing to neuronal loss in neurodegenerative disorders [96–98].

GO categories related to cyclin-dependent kinases (CDKs) were significantly associated with cortical thickness. CDKs regulate cellular process and play an important role in the nervous system [92–93]. CDK pathways involved the aberrant reactivation of the cell cycle and neuronal differentiation contribute to the neuronal loss that is responsible for AD [101]. CDK5, a component of CDKs, was reported to play roles in neuronal migration, differentiation, and synaptic functions [102]. Moreover, regulated CDK5 phosphorylates serine or threonine sites on substrate proteins associated with cortex layer formation, and CDK5 contributes to multiple steps of cortical neuronal migration [90, 103, 104]. In this study, we reported 28 genes in two significant pathways associated with cortical thickness. Among them, five genes have been reported to be associated with AD. Thus, pathways related to CDKs may influence the cortical thickness, as well as AD.

This study has several limitations. ADNI is an observational, multi-center study of AD progression, and the nature of our sample makes it difficult to generalize our findings to other populations. Thus, further analyses in independent larger community studies with diverse populations are required to investigate our findings. Although we used neuroimaging-based endophenotypes and genetic data from publicly available ADNI datasets to perform this study, our sample size is moderate, and we could not use a replication data. Thus, replication of our findings in larger independent data is warranted. A thinning of the brain cortex has been demonstrated in many brain disorders such as stroke and depression. However, in ADNI, according to inclusion and exclusion criteria, participants with history of structural brain lesion, major depression, head trauma, and significant neurological diseases other than AD were excluded [105].

In this gene-based association analysis, we identified new associations of genes with mean cortical thickness that were not identified in SNP-based GWAS. This method is complementary technique for SNP-based GWAS. The gene-based p-values reflect the effect of entire gene and would not necessarily reach strict genome-wide significance level. Additional eQTL and vertex-wise association analysis confirmed the importance of intronic SNPs mapped to identified genes from gene-based association analysis. According to our additional eQTL and vertex-wise association analysis, intronic SNPs of identified genes have impact on gene expression and cortical thickness of AD-related brain regions. The PPI network and pathway analysis allow us to confirm effect of functionally related genes and found one PPI pair and two pathways. The advantage of this study design allows us to determine complementary information using the structures of genomic data and gain valuable insight into genetic networks of functionally related genes.

In conclusion, by taking the advantage of gene-based, PPI network, and pathway enrichment analysis methods to perform complementary analysis of SNP-based GWAS, we identified novel genes as significantly associated with mean cortical thickness in AD. Our findings based on an imaging genetics approach to use MRI-based measures as an endophenotype for genetic studies will provide new insights into the biological mechanisms of AD pathogenesis.

ACKNOWLEDGMENTS

This work was supported by the National Research Foundation of Korea (NRF) grant funded by the Korea government (MSIT) (NRF-5942019R1H1A2101514), Korea Health Technology R&D Project through the Korea Health Industry Development Institute (KHIDI), funded by the Ministry of Health & Welfare, Republic of Korea

(grant number: HI19C1234), NLM R01 LM012535, NIA 595R03 AG054936, and NIA R03 AG063250.

Data collection and sharing for this project was funded by the Alzheimer's Disease Neuroimaging Initiative (ADNI) (National Institutes of Health Grant U01 AG024904) and DOD ADNI (Department of Defense award number W81XWH-12-2-0012). ADNI is funded by the National Institute on Aging, the National Institute of Biomedical Imaging and Bioengineering, and through generous contributions from the following: AbbVie, Alzheimer's Association; Alzheimer's Drug Discovery Foundation; Araclon Biotech; BioClinica, Inc.; Biogen; Bristol-Myers Squibb Company; CereSpir, Inc.; Cogstate; Eisai Inc.; Elan Pharmaceuticals, Inc.; Eli Lilly and Company; EuroImmun; F. Hoffmann-La Roche Ltd and its affiliated company Genentech, Inc.; Fujirebio; GE Healthcare; IXICO Ltd.; Janssen Alzheimer Immunotherapy Research & Development, LLC.; Johnson & Johnson Pharmaceutical Research & Development LLC.; Lumosity; Lundbeck; Merck & Co., Inc.; Meso Scale Diagnostics, LLC.; NeuroRx Research; Neurotrack Technologies; Novartis Pharmaceuticals Corporation; Pfizer Inc.; Piramal Imaging; Servier; Takeda Pharmaceutical Company; and Transition Therapeutics. The Canadian Institutes of Health Research is providing funds to support ADNI clinical sites in Canada. Private sector contributions are facilitated by the Foundation for the National Institutes of Health (http://www.fnih.org). The grantee organization is the Northern California Institute for Research and Education, and the study is coordinated by the Alzheimer's Therapeutic Research Institute at the University of Southern California. ADNI data are disseminated by the Laboratory for Neuro Imaging at the University of Southern California.

Authors' disclosures available online (https://www.j-alz.com/manuscript-disclosures/19-1175r1).

SUPPLEMENTARY MATERIAL

The supplementary material is available in the electronic version of this article: http://dx.doi.org/10.3233/JAD-191175.

REFERENCES

[1] Karch CM, Cruchaga C, Goate AM (2014) Alzheimer's disease genetics: From the bench to the clinic. *Neuron* **83**, 11-26.

[2] Gatz M, Reynolds CA, Fratiglioni L, Johansson B, Mortimer JA, Berg S, Fiske A, Pedersen NL (2006) Role of genes and environments for explaining Alzheimer disease. *Arch Gen Psychiatry* **63**, 168.

[3] Corder E, Saunders A, Strittmatter W, Schmechel D, Gaskell P, Small G, Roses A, Haines J, Pericak-Vance M (1993) Gene dose of apolipoprotein E type 4 allele and the risk of Alzheimer's disease in late onset families. *Science* **261**, 921-923.

[4] Saunders AM, Strittmatter WJ, Schmechel D, St. George-Hyslop PH, Pericak-Vance MA, Joo SH, Rosi BL, Gusella JF, Crapper-MacLachlan DR, Alberts MJ, Hulette C, Crain B, Goldgaber D, Roses AD (1993) Association of apolipoprotein E allele 4 with late-onset familial and sporadic Alzheimer's disease. *Neurology* **43**, 1467-1467.

[5] Jun G (2010) Meta-analysis Confirms CR1, CLU, and PICALM as Alzheimer Disease Risk Loci and Reveals Interactions with APOE Genotypes. *Arch Neurol* **67**, 1473.

[6] Lambert JC, Ibrahim-Verbaas CA, Harold D, Naj AC, Sims R, Bellenguez C, Jun G, DeStefano AL, Bis JC, Beecham GW, Grenier-Boley B, Russo G, Thornton-Wells TA, Jones N, Smith AV, Chouraki V, Thomas C, Ikram MA, Zelenika D, Vardarajan BN, Kamatani Y, Lin CF, Gerrish A, Schmidt H, Kunkle B, Fiévet N, Amouyel P, Pasquier F, Deramecourt V, De Bruijn RFAG, Amin N, Hofman A, Van Duijn CM, Dunstan ML, Hollingworth P, Owen MJ, O'Donovan MC, Jones L, Holmans PA, Moskvina V, Williams J, Baldwin C, Farrer LA, Choi SH, Lunetta KL, Fitzpatrick AL, Harris TB, Psaty BM, Gilbert JR, Hamilton-Nelson KL, Martin ER, Pericak-Vance MA, Haines JL, Gudnason V, Jonsson PV, Eiriksdottir G, Bihoreau MT, Lathrop M, Valladares O, Cantwell LB, Wang LS, Schellenberg GD, Ruiz A, Boada M, Reitz C, Mayeux R, Ramirez A, Maier W, Hanon O, Kukull WA, Buxbaum JD, Campion D, Wallon D, Hannequin D, Crane PK, Larson EB, Becker T, Cruchaga C, Goate AM, Craig D, Johnston JA, Mc-Guinness B, Todd S, Passmore P, Berr C, Ritchie K, Lopez OL, De Jager PL, Evans D, Lovestone S, Proitsi P, Powell JF, Letenneur L, Barberger-Gateau P, Dufouil C, Dartigues JF, Morón FJ, Rubinsztein DC, St. George-Hyslop P, Sleegers K, Bettens K, Van Broeckhoven C, Huentelman MJ, Gill M, Brown K, Morgan K, Kamboh MI, Keller L, Fratiglioni L, Green R, Myers AJ, Love S, Rogaeva E, Gallacher J, Bayer A, Clarimon J, Lleo A, Tsuang DW, Yu L, Bennett DA, Tsolaki M, Bossù P, Spalletta G, Collinge J, Mead S, Sorbi S, Nacmias B, Sanchez-Garcia F, Deniz Naranjo MC, Fox NC, Hardy J, Bosco P, Clarke R, Brayne C, Galimberti D, Mancuso M, Matthews F, Moebus S, Mecocci P, Del Zompo M, Hampel H, Pilotto A, Bullido M, Panza F, Caffarra P, Mayhaus M, Pichler S, Gu W, Riemenschneider M, Lannfelt L, Ingelsson M, Hakonarson H, Carrasquillo MM, Zou F, Younkin SG, Beekly D, Alvarez V, Coto E, Razquin C, Pastor P, Mateo I, Combarros O, Faber KM, Foroud TM, Soininen H, Hiltunen M, Blacker D, Mosley TH, Graff C, Holmes C, Montine TJ, Rotter JI, Brice A, Nalls MA, Kauwe JSK, Boerwinkle E, Schmidt R, Rujescu D, Tzourio C, Nöthen MM, Launer LJ, Seshadri S (2013) Meta-analysis of 74,046 individuals identifies 11 new susceptibility loci for Alzheimer's disease. *Nat Genet* **45**, 1452-1458.

[7] Wang HF, Wan Y, Hao XK, Cao L, Zhu XC, Jiang T, Tan MS, Tan L, Zhang DQ, Tan L, Yu JT (2016) Bridging Integrator 1 (BIN1) genotypes mediate Alzheimer's dis-

ease risk by altering neuronal degeneration. *J Alzheimers Dis* **52**, 179-190.

[8] Manolio TA, Collins FS, Cox NJ, Goldstein DB, Hindorff LA, Hunter DJ, McCarthy MI, Ramos EM, Cardon LR, Chakravarti A, Cho JH, Guttmacher AE, Kong A, Kruglyak L, Mardis E, Rotimi CN, Slatkin M, Valle D, Whittemore AS, Boehnke M, Clark AG, Eichler EE, Gibson G, Haines JL, MacKay TFC, McCarroll SA, Visscher PM (2009) Finding the missing heritability of complex diseases. *Nature* **461**, 747-753.

[9] Sandoval-Motta S, Aldana M, Martínez-Romero E, Frank A (2017) The human microbiome and the missing heritability problem. *Front Genet* **8**, 1-12.

[10] Marian AJ (2012) Elements of "missing heritability." *Curr Opin Cardiol* **27**, 197-201.

[11] Zuk O, Hechter E, Sunyaev SR, Lander ES (2012) The mystery of missing heritability: Genetic interactions create phantom heritability. *Proc Natl Acad Sci U S A* **109**, 1193-1198.

[12] Slatkin M (2009) Epigenetic inheritance and the missing heritability problem. *Genetics* **182**, 845-850.

[13] Blanco-Gómez A, Castillo-Lluva S, del Mar Sáez-Freire M, Hontecillas-Prieto L, Mao JH, Castellanos-Martín A, Pérez-Losada J (2016) Missing heritability of complex diseases: Enlightenment by genetic variants from intermediate phenotypes. *Bioessays* **38**, 664-673.

[14] Braskie MN, Ringman JM, Thompson PM (2011) Neuroimaging measures as endophenotypes in Alzheimer's disease. *Int J Alzheimers Dis* **2011**, 490140.

[15] Manchia M, Cullis J, Turecki G, Rouleau GA, Uher R, Alda M (2013) The impact of phenotypic and genetic heterogeneity on results of genome wide association studies of complex diseases. *PLoS One* **8**, e76295.

[16] Meyer-Lindenberg A, Weinberger DR (2006) Intermediate phenotypes and genetic mechanisms of psychiatric disorders. *Nat Rev Neurosci* **7**, 818-827.

[17] Lenzenweger MF (2013) Endophenotype, intermediate phenotype, biomarker: Definitions, concept comparisons, clarifications. *Depress Anxiety* **30**, 185-189.

[18] Leboyer M, Bellivier F, Jouvent R, Nosten-Bertrand M, Mallet J, Pauls D (1998) Psychiatric genetics: Search for phenotypes. *Trends Neurosci* **21**, 102-105.

[19] Lenzenweger MF (2013) Thinking clearly about the endophenotype-intermediate phenotype-biomarker distinctions in developmental psychopathology research. *Dev Psychopathol* **25**, 1347-1357.

[20] Gottesman II, Gould TD (2003) The endophenotype concept in psychiatry: Etymology and strategic intentions. *Am J Psychiatry* **160**, 636-645.

[21] Hashimoto R, Ohi K, Yamamori H, Yasuda Y, Fujimoto M, Umeda-Yano S, Watanabe Y, Fukunaga M, Takeda M (2015) Imaging genetics and psychiatric disorders. *Curr Mol Med* **15**, 168-175.

[22] Potkin SG, Guffanti G, Lakatos A, Turner JA, Kruggel F, Fallon JH, Saykin AJ, Orro A, Lupoli S, Salvi E, Weiner M, Macciardi F (2009) Hippocampal atrophy as a quantitative trait in a genome-wide association study identifying novel susceptibility genes for Alzheimer's disease. *PLoS One* **4**, e6501.

[23] Bakken TE, Bloss CS, Roddey JC, Joyner AH, Rimol LM, Djurovic S, Melle I, Sundet K, Agartz I, Andreassen OA, Dale AM, Schork NJ (2011) Association of genetic variants on 15q12 with cortical thickness and cognition in schizophrenia. *Arch Gen Psychiatry* **68**, 781-790.

[24] Matsushita T, Madireddy L, Sprenger T, Khankhanian P, Magon S, Naegelin Y, Caverzasi E, Lindberg RLP, Kappos L, Hauser SL, Oksenberg JR, Henry R, Pelletier D, Baranzini SE (2015) Genetic associations with brain cortical thickness in multiple sclerosis. *Genes Brain Behav* **14**, 217-227.

[25] Ramanan VK, Risacher SL, Nho K, Kim S, Shen L, McDonald BC, Yoder KK, Hutchins GD, West JD, Tallman EF, Gao S, Foroud TM, Farlow MR, De Jager PL, Bennett DA, Aisen PS, Petersen RC, Jack CR, Toga AW, Green RC, Jagust WJ, Weiner MW, Saykin AJ (2015) GWAS of longitudinal amyloid accumulation on18F-florbetapir PET in Alzheimer's disease implicates microglial activation gene IL1RAP. *Brain* **138**, 3076-3088.

[26] Pini L, Pievani M, Bocchetta M, Altomare D, Bosco P, Cavedo E, Galluzzi S, Marizzoni M, Frisoni GB (2016) Brain atrophy in Alzheimer's disease and aging. *Ageing Res Rev* **30**, 25-48.

[27] Kale VV, Hamde ST, Holambe RS (2019) Multi class disorder detection of magnetic resonance brain images using composite features and neural network. *Biomed Eng Lett* **9**, 221-231.

[28] Shen L, Kim S, Risacher SL, Nho K, Swaminathan S, West JD, Foroud T, Pankratz N, Moore JH, Sloan CD, Huentelman MJ, Craig DW, DeChairo BM, Potkin SG, Jack CR, Weiner MW, Saykin AJ (2010) Whole genome association study of brain-wide imaging phenotypes for identifying quantitative trait loci in MCI and AD: A study of the ADNI cohort. *Neuroimage* **53**, 1051-1063.

[29] Hibar DP, Stein JL, Renteria ME, Arias-Vasquez A, Desrivières S, Jahanshad N, Toro R, Wittfeld K, Abramovic L, Andersson M, Aribisala BS, Armstrong NJ, Bernard M, Bohlken MM, Boks MP, Bralten J, Brown AA, Mallar Chakravarty M, Chen Q, Ching CRK, Cuellar-Partida G, Den Braber A, Giddaluru S, Goldman AL, Grimm O, Guadalupe T, Hass J, Woldehawariat G, Holmes AJ, Hoogman M, Janowitz D, Jia T, Kim S, Klein M, Kraemer B, Lee PH, Olde Loohuis LM, Luciano M, MacAre C, Mather KA, Mattheisen M, Milaneschi Y, Nho K, Papmeyer M, Ramasamy A, Risacher SL, Roiz-Santiañez R, Rose EJ, Salami A, Sämann PG, Schmaal L, Schork AJ, Shin J, Strike LT, Teumer A, Van Donkelaar MMJ, Van Eijk KR, Walters RK, Westlye LT, Whelan CD, Winkler AM, Zwiers MP, Alhusaini S, Athanasiu L, Ehrlich S, Hakobjan MMH, Hartberg CB, Haukvik UK, Heister AJGAM, Hoehn D, Kasperaviciute D, Liewald DCM, Lopez LM, Makkinje RRR, Matarin M, Naber MAM, Reese McKay D, Needham M, Nugent AC, Pütz B, Royle NA, Shen L, Sprooten E, Trabzuni D, Van Der Marel SSL, Van Hulzen KJE, Walton E, Wolf C, Almasy L, Ames D, Arepalli S, Assareh AA, Bastin ME, Brodaty H, Bulayeva KB, Carless MA, Cichon S, Corvin A, Curran JE, Czisch M, De Zubicaray GI, Dillman A, Duggirala R, Dyer TD, Erk S, Fedko IO, Ferrucci L, Foroud TM, Fox PT, Fukunaga M, Raphael Gibbs J, Göring HHH, Green RC, Guelfi S, Hansell NK, Hartman CA, Hegenscheid K, Heinz A, Hernandez DG, Heslenfeld DJ, Hoekstra PJ, Holsboer F, Homuth G, Hottenga JJ, Ikeda M, Jack CR, Jenkinson M, Johnson R, Kanai R, Keil M, Kent JW, Kochunov P, Kwok JB, Lawrie SM, Liu X, Longo DL, McMahon KL, Meisenzahl E, Melle I, Mohnke S, Montgomery GW, Mostert JC, Mühleisen TW, Nalls MA, Nichols TE, Nilsson LG, Nöthen MM, Ohi K, Olvera RL, Perez-Iglesias R, Bruce Pike G, Potkin SG, Reinvang I, Reppermund S,

Rietschel M, Romanczuk-Seiferth N, Rosen GD, Rujescu D, Schnell K, Schofield PR, Smith C, Steen VM, Sussmann JE, Thalamuthu A, Toga AW, Traynor BJ, Troncoso J, Turner JA, Valdés Hernández MC, Van 'T Ent D, Van Der Brug M, Van Der Wee NJA, Van Tol MJ, Veltman DJ, Wassink TH, Westman E, Zielke RH, Zonderman AB, Ashbrook DG, Hager R, Lu L, McMahon FJ, Morris DW, Williams RW, Brunner HG, Buckner RL, Buitelaar JK, Cahn W, Calhoun VD, Cavalleri GL, Crespo-Facorro B, Dale AM, Davies GE, Delanty N, Depondt C, Djurovic S, Drevets WC, Espeseth T, Gollub RL, Ho BC, Hoffmann W, Hosten N, Kahn RS, Le Hellard S, Meyer-Lindenberg A, Müller-Myhsok B, Nauck M, Nyberg L, Pandolfo M, Penninx BWJH, Roffman JL, Sisodiya SM, Smoller JW, Van Bokhoven H, Van Haren NEM, Völzke H, Walter H, Weiner MW, Wen W, White T, Agartz I, Andreassen OA, Blangero J, Boomsma DI, Brouwer RM, Cannon DM, Cookson MR, De Geus EJC, Deary IJ, Donohoe G, Fernández G, Fisher SE, Francks C, Glahn DC, Grabe HJ, Gruber O, Hardy J, Hashimoto R, Hulshoff Pol HE, Jönsson EG, Kloszewska I, Lovestone S, Mattay VS, Mecocci P, McDonald C, McIntosh AM, Ophoff RA, Paus T, Pausova Z, Ryten M, Sachdev PS, Saykin AJ, Simmons A, Singleton A, Soininen H, Wardlaw JM, Weale ME, Weinberger DR, Adams HHH, Launer LJ, Seiler S, Schmidt R, Chauhan G, Satizabal CL, Becker JT, Yanek L, Van Der Lee SJ, Ebling M, Fischl B, Longstreth WT, Greve D, Schmidt H, Nyquist P, Vinke LN, Van Duijn CM, Xue L, Mazoyer B, Bis JC, Gudnason V, Seshadri S, Ikram MA, Martin NG, Wright MJ, Schumann G, Franke B, Thompson PM, Medland SE (2015) Common genetic variants influence human subcortical brain structures. *Nature* **520**, 224-229.

[30] Querbes O, Aubry F, Pariente J, Lotterie J-A, Démonet J-F, Duret V, Puel M, Berry I, Fort J-C, Celsis P (2009) Early diagnosis of Alzheimer's disease using cortical thickness: Impact of cognitive reserve. *Brain* **132**, 2036-2047.

[31] Braak H, Braak E (1991) Neuropathological staging of Alzheimer-related changes. *Acta Neuropathol* **82**, 239-259.

[32] Dickerson BC, Bakkour A, Salat DH, Feczko E, Pacheco J, Greve DN, Grodstein F, Wright CI, Blacker D, Rosas HD, Sperling RA, Atri A, Growdon JH, Hyman BT, Morris JC, Fischl B, Buckner RL (2009) The cortical signature of Alzheimer's disease9 Regionally specific cortical thinning relates to symptom severity in very mild to mild AD dementia and is detectable in asymptomatic amyloid-positive individuals. *Cereb Cortex* **19**, 497-510.

[33] Lerch JP, Pruessner JC, Zijdenbos A, Hampel H, Teipel SJ, Evans AC (2005) Focal decline of cortical thickness in Alzheimer's disease identified by computational neuroanatomy. *Cereb Cortex* **15**, 995-1001.

[34] Du A-T, Schuff N, Kramer JH, Rosen HJ, Gorno-Tempini ML, Rankin K, Miller BL, Weiner MW (2007) Different regional patterns of cortical thinning in Alzheimer's disease and frontotemporal dementia. *Brain* **130**, 1159-1166.

[35] Winkler AM, Kochunov P, Blangero J, Almasy L, Zilles K, Fox PT, Duggirala R, Glahn DC (2010) Cortical thickness or grey matter volume? The importance of selecting the phenotype for imaging genetics studies. *Neuroimage* **53**, 1135-1146.

[36] Furney SJ, Simmons a, Breen G, Pedroso I, Lunnon K, Proitsi P, Hodges A, Powell J, Wahlund L-O, Kloszewska I, Mecocci P, Soininen H, Tsolaki M, Vellas B, Spenger C, Lathrop M, Shen L, Kim S, Saykin AJ, Weiner MW, Lovestone S (2011) Genome-wide association with MRI atrophy measures as a quantitative trait locus for Alzheimer's disease. *Mol Psychiatry* **16**, 1130-1138.

[37] Wolthusen RPF, Hass J, Walton E, Turner JA, Rössner V, Sponheim SR, Ho B-C, Holt DJ, Gollub RL, Calhoun V, Ehrlich S (2015) Genetic underpinnings of left superior temporal gyrus thickness in patients with schizophrenia. *World J Biol Psychiatry* **2975**, 1-11.

[38] Li MX, Gui HS, Kwan JSH, Sham PC (2011) GATES: A rapid and powerful gene-based association test using extended Simes procedure. *Am J Hum Genet* **88**, 283-293.

[39] Wang L, Jia P, Wolfinger RD, Chen X, Zhao Z (2011) Gene set analysis of genome-wide association studies: Methodological issues and perspectives. *Genomics* **98**, 1–8.

[40] Jorgenson E, Witte JS (2006) A gene-centric approach to genome-wide association studies. *Nat Rev Genet* **7**, 885-891.

[41] Neale BM, Sham PC (2004) The future of association studies: Gene-based analysis and replication. *Am J Hum Genet* **75**, 353-362.

[42] Mo X, Lu X, Zhang Y, Zhang Z, Deng F, Lei S (2015) Gene-based association analysis identified novel genes associated with bone mineral density. *PLoS One* **10**, e0121811.

[43] Mukherjee S, Kim S, Ramanan VK, Gibbons LE, Nho K, Glymour MM, Ertekin-Taner N, Montine TJ, Saykin AJ, Crane PK (2014) Gene-based GWAS and biological pathway analysis of the resilience of executive functioning. *Brain Imag Behav* **8**, 110-118.

[44] Peng G, Luo L, Siu H, Zhu Y, Hu P, Hong S, Zhao J, Zhou X, Reveille JD, Jin L, Amos CI, Xiong M (2010) Gene and pathway-based second-wave analysis of genome-wide association studies. *Eur J Hum Genet* **18**, 111-117.

[45] Holmans P (2010) Statistical methods for pathway analysis of genome-wide data for association with complex genetic traits. *Adv Genet* **72**, 141-179.

[46] Kendler KS, Neale MC (2010) Endophenotype: A conceptual analysis. *Mol Psychiatry* **15**, 789-797.

[47] Bai F, Yuan Y, Shi Y, Zhang Z (2016) Multiple genetic imaging study of the association between cholesterol metabolism and brain functional alterations in individuals with risk factors for Alzheimer's disease. *Oncotarget* **7**, 15315-15328.

[48] Jack CR, Bernstein MA, Fox NC, Thompson P, Alexander G, Harvey D, Borowski B, Britson PJ, Whitwell JL, Ward C, Dale AM, Felmlee JP, Gunter JL, Hill DLG, Killiany R, Schuff N, Fox-Bosetti S, Lin C, Studholme C, DeCarli CS, Krueger G, Ward HA, Metzger GJ, Scott KT, Mallozzi R, Blezek D, Levy J, Debbins JP, Fleisher AS, Albert M, Green R, Bartzokis G, Glover G, Mugler J, Weiner MW (2008) The Alzheimer's Disease Neuroimaging Initiative (ADNI): MRI methods. *J Magn Reson Imag* **27**, 685-691.

[49] Mueller SG, Weiner MW, Thal LJ, Petersen RC, Jack C, Jagust W, Trojanowski JQ, Toga AW, Beckett L (2005) The Alzheimer's disease neuroimaging initiative. *Neuroimag Clin N Am* **15**, 869-877.

[50] Mueller SG, Weiner MW, Thal LJ, Petersen RC, Jack CR, Jagust W, Trojanowski JQ, Toga AW, Beckett L (2005) Ways toward an early diagnosis in Alzheimer's disease: The Alzheimer's Disease Neuroimaging Initiative (ADNI). *Alzheimers Dement* **1**, 55-66.

[51] Sled JG, Zijdenbos AP, Evans AC (1998) A nonparametric method for automatic correction of intensity nonuniformity in MRI data. *IEEE Trans Med Imag* **17**, 87-97.

[52] Collins DL, Neelin P, Peters TM, Evans AC (1994) Automatic 3D intersubject registration of MR volumetric data in standardized Talairach space. *J Comput Assist Tomogr* **18**, 192-205.

[53] Zijdenbos A, Evans A, Riahi F, Sled J, Chui J, Kollokian V (1996) Automatic quantification of multiple sclerosis lesion volume using stereotaxic space. *Vis Biomed Comput* **1131**, 439-448.

[54] MacDonald D, Kabani N, Avis D, Evans AC (2000) Automated 3-D extraction of inner and outer surfaces of cerebral cortex from MRI. *Neuroimage* **12**, 340-356.

[55] June SK, Singh V, Jun KL, Lerch J, Ad-Dab'bagh Y, MacDonald D, Jong ML, Kim SI, Evans AC (2005) Automated 3-D extraction and evaluation of the inner and outer cortical surfaces using a Laplacian map and partial volume effect classification. *Neuroimage* **27**, 210-221.

[56] Lerch JP, Evans AC (2005) Cortical thickness analysis examined through power analysis and a population simulation. *Neuroimage* **24**, 163-173.

[57] Saykin AJ, Shen L, Foroud TM, Potkin SG, Swaminathan S, Kim S, Risacher SL, Nho K, Huentelman MJ, Craig DW, Thompson PM, Stein JL, Moore JH, Farrer LA, Green RC, Bertram L, Jack CR, Weiner MW (2010) Alzheimer's Disease Neuroimaging Initiative biomarkers as quantitative phenotypes: Genetics core aims, progress, and plans. *Alzheimers Dement* **6**, 265-273.

[58] Saykin AJ, Shen L, Yao X, Kim S, Nho K, Risacher SL, Ramanan VK, Foroud TM, Faber KM, Sarwar N, Munsie LM, Hu X, Soares HD, Potkin SG, Thompson PM, Kauwe JSK, Kaddurah-Daouk R, Green RC, Toga AW, Weiner MW (2015) Genetic studies of quantitative MCI and AD phenotypes in ADNI: Progress, opportunities, and plans. *Alzheimers Dement* **11**, 792-814.

[59] Marchini J, Howie B, Myers S, McVean G, Donnelly P (2007) A new multipoint method for genome-wide association studies by imputation of genotypes. *Nat Genet* **39**, 906-913.

[60] Genomes Project Consortium T 1000 GP, Abecasis GR, Auton A, Brooks LD, DePristo MA, Durbin RM, Handsaker RE, Kang HM, Marth GT, McVean GA (2012) An integrated map of genetic variation from 1,092 human genomes. *Nature* **491**, 56-65.

[61] Purcell S, Neale B, Todd-Brown K, Thomas L, Ferreira MAR, Bender D, Maller J, Sklar P, de Bakker PIW, Daly MJ, Sham PC (2007) PLINK: A tool set for whole-genome association and population-based linkage analyses. *Am J Hum Genet* **81**, 559-575.

[62] Price AL, Zaitlen NA, Reich D, Patterson N (2010) New approaches to population stratification in genome-wide association studies. *Nat Rev Genet* **11**, 459-463.

[63] Schwarz CG, Gunter JL, Wiste HJ, Przybelski SA, Weigand SD, Ward CP, Senjem ML, Vemuri P, Murray ME, Dickson DW, Parisi JE, Kantarci K, Weiner MW, Petersen RC, Jack CR (2016) A large-scale comparison of cortical thickness and volume methods for measuring Alzheimer's disease severity. *Neuroimage Clin* **11**, 802-812.

[64] Barnes J, Ridgway GR, Bartlett J, Henley SMD, Lehmann M, Hobbs N, Clarkson MJ, MacManus DG, Ourselin S, Fox NC (2010) Head size, age and gender adjustment in MRI studies: A necessary nuisance? *Neuroimage* **53**, 1244-1255.

[65] Zhao K, Liu H, Yan R, Hua L, Chen Y, Shi J, Lu Q, Yao Z (2017) Cortical thickness and subcortical structure volume abnormalities in patients with major depression with and without anxious symptoms. *Brain Behav* **7**, e00754.

[66] Hochberg B (1995) Controlling the false discovery rate: A practical and powerful approach to multiple testing. *J R Stat Soc* **57**, 289-300.

[67] Ramasamy A, Trabzuni D, Guelfi S, Varghese V, Smith C, Walker R, De T, Coin L, De Silva R, Cookson MR, Singleton AB, Hardy J, Ryten M, Weale ME (2014) Genetic variability in the regulation of gene expression in ten regions of the human brain. *Nat Neurosci* **17**, 1418-1428.

[68] Szklarczyk D, Morris JH, Cook H, Kuhn M, Wyder S, Simonovic M, Santos A, Doncheva NT, Roth A, Bork P, Jensen LJ, Von Mering C (2017) The STRING database in 2017: Quality-controlled protein-protein association networks, made broadly accessible. *Nucleic Acids Res* **45**, D362-D368.

[69] Li MX, Kwan JSH, Sham PC (2012) HYST: A hybrid set-based test for genome-wide association studies, with application to protein-protein interaction-based association analysis. *Am J Hum Genet* **91**, 478-488.

[70] Higgins JPT, Thompson SG, Deeks JJ, Altman DG (2003) Measuring inconsistency in meta-analyses. *BMJ Br Med J* **327**, 557-560.

[71] Elbers CC, van Eijk KR, Franke L, Mulder F, van der Schouw YT, Wijmenga C, Onland-Moret NC (2009) Using genome-wide pathway analysis to unravel the etiology of complex diseases. *Genet Epidemiol* **33**, 419-431.

[72] Yu W, Clyne M, Khoury MJ, Gwinn M (2009) Phenopedia and genopedia: Disease-centered and gene-centered views of the evolving knowledge of human genetic associations. *Bioinformatics* **26**, 145-146.

[73] Ariga T, Wakade C, Yu RK (2011) The pathological roles of ganglioside metabolism in Alzheimer's disease: Effects of gangliosides on neurogenesis. *Int J Alzheimers Dis* **2011**, 1-14.

[74] Palmano K, Rowan A, Guillermo R, Guan J, McJarrow P (2015) The role of gangliosides in neurodevelopment. *Nutrients* **7**, 3891-3913.

[75] Ohmi Y, Tajima O, Ohkawa Y, Mori A, Sugiura Y, Furukawa K, Furukawa K (2009) Gangliosides play pivotal roles in the regulation of complement systems and in the maintenance of integrity in nerve tissues. *Proc Natl Acad Sci U S A* **106**, 22405-22410.

[76] Yu RK, Nakatani Y, Yanagisawa M (2009) The role of glycosphingolipid metabolism in the developing brain. *J Lipid Res* **50**, S440-S445.

[77] Yanagisawa K, Ihara Y (1998) GM1 ganglioside-bound amyloid beta-protein in Alzheimer's disease brain. *Neurobiol Aging* **19**, S65-67.

[78] Sheikh KA, Sun J, Liu Y, Kawai H, Crawford TO, Proia RL, Griffin JW, Schnaar RL (1999) Mice lacking complex gangliosides develop Wallerian degeneration and myelination defects. *Proc Natl Acad Sci U S A* **96**, 7532-7537.

[79] Harlalka GV, Lehman A, Chioza B, Baple EL, Maroofian R, Cross H, Sreekantan-Nair A, Priestman DA, Al-Turki S, McEntagart ME, Proukakis C, Royle L, Kozak RP, Bastaki L, Patton M, Wagner K, Coblentz R, Price J, Mezei M, Schlade-Bartusiak K, Platt FM, Hurles ME, Crosby AH (2013) Mutations in B4GALNT1 (GM2 synthase) underlie a new disorder of ganglioside biosynthesis. *Brain* **136**(Pt 12), 3618-3624.

[80] Kalanj S, Kracun I, Rosner H, Cosović C (1991) Regional distribution of brain gangliosides in Alzheimer's disease. *Neurol Croat* **40**, 269-281.

[81] Kracun I, Kalanj S, Cosovic C, Talan-Hranilovic J (1990) Brain gangliosides in Alzheimer's disease. *J Hirnforsch* **31**, 789-793.

[82] Kracun I, Kalanj S, Talan-Hranilovic J, Cosovic C (1992) Cortical distribution of gangliosides in Alzheimer's disease. *Neurochem Int* **20**, 433-438.

[83] Chiavegatto S, Sun J, Nelson RJ, Schnaar RL (2000) A functional role for complex gangliosides: Motor deficits in GM2/GD2 synthase knockout mice. *Exp Neurol* **166**, 227-234.

[84] Bhuiyan RH, Ohmi Y, Ohkawa Y, Zhang P, Takano M, Hashimoto N, Okajima T, Furukawa K, Furukawa K (2019) Loss of enzyme activity in mutated B4GALNT1 gene products in patients with hereditary spastic paraplegia results in relatively mild neurological disorders: Similarity with phenotypes of B4galnt1 knockout mice. *Neuroscience* **397**, 94-106.

[85] Yamaguchi T, Yamauchi Y, Furukawa K, Ohmi Y, Ohkawa Y, Zhang Q, Okajima T, Furukawa K (2016) Expression of B4GALNT1, an essential glycosyltransferase for the synthesis of complex gangliosides, suppresses BACE1 degradation and modulates APP processing. *Sci Rep* **6**, 1-12.

[86] Udayar V, Buggia-Prévot V, Guerreiro RL, Siegel G, Rambabu N, Soohoo AL, Ponnusamy M, Siegenthaler B, Bali J, Simons M, Ries J, Puthenveedu MA, Hardy J, Thinakaran G, Rajendran L (2013) A Paired RNAi and RabGAP overexpression screen identifies Rab11 as a regulator of β-amyloid production. *Cell Rep* **5**, 1536-1551.

[87] Li G (2011) Rab GTPases, membrane trafficking and diseases. *Curr Drug Targets* **12**, 1188-1193.

[88] Ginsberg SD, Alldred MJ, Counts SE, Cataldo AM, Neve RL, Jiang Y, Wuu J, Chao MV, Mufson EJ, Nixon RA, Che S (2010) Microarray analysis of hippocampal CA1 neurons implicates early endosomal dysfunction during Alzheimer's disease progression. *Biol Psychiatry* **68**, 885-893.

[89] Cataldo AM, Peterhoff CM, Troncoso JC, Gomez-Isla T, Hyman BT, Nixon RA (2000) Endocytic pathway abnormalities precede amyloid β deposition in sporadic Alzheimer's disease and down syndrome: Differential effects of APOE genotype and presenilin mutations. *Am J Pathol* **157**, 277-286.

[90] Kawauchi T, Sekine K, Shikanai M, Chihama K, Tomita K, Kubo K ichiro, Nakajima K, Nabeshima Y ichi, Hoshino M (2010) Rab GTPases-dependent endocytic pathways regulate neuronal migration and maturation through N-cadherin trafficking. *Neuron* **67**, 588-602.

[91] Herold C, Hooli BV, Mullin K, Liu T, Roehr JT, Mattheisen M, Parrado AR, Bertram L, Lange C, Tanzi RE (2016) Family-based association analyses of imputed genotypes reveal genome-wide significant association of Alzheimer's disease with OSBPL6, PTPRG, and PDCL3. *Mol Psychiatry* **21**, 1608-1612.

[92] Naj AC, Jun G, Beecham GW, Wang L-S, Vardarajan BN, Buros J, Gallins PJ, Buxbaum JD, Jarvik GP, Crane PK, Larson EB, Bird TD, Boeve BF, Graff-Radford NR, De Jager PL, Evans D, Schneider JA, Carrasquillo MM, Ertekin-Taner N, Younkin SG, Cruchaga C, Kauwe JSK, Nowotny P, Kramer P, Hardy J, Huentelman MJ, Myers AJ, Barmada MM, Demirci FY, Baldwin CT, Green RC, Rogaeva E, St George-Hyslop P, Arnold SE, Barber R, Beach T, Bigio EH, Bowen JD, Boxer A, Burke JR, Cairns NJ, Carlson CS, Carney RM, Carroll SL, Chui HC, Clark DG, Corneveaux J, Cotman CW, Cummings JL, DeCarli C, DeKosky ST, Diaz-Arrastia R, Dick M, Dickson DW, Ellis WG, Faber KM, Fallon KB, Farlow MR, Ferris S, Frosch MP, Galasko DR, Ganguli M, Gearing M, Geschwind DH, Ghetti B, Gilbert JR, Gilman S, Giordani B, Glass JD, Growdon JH, Hamilton RL, Harrell LE, Head E, Honig LS, Hulette CM, Hyman BT, Jicha GA, Jin L-W, Johnson N, Karlawish J, Karydas A, Kaye JA, Kim R, Koo EH, Kowall NW, Lah JJ, Levey AI, Lieberman AP, Lopez OL, Mack WJ, Marson DC, Martiniuk F, Mash DC, Masliah E, McCormick WC, McCurry SM, McDavid AN, McKee AC, Mesulam M, Miller BL, Miller CA, Miller JW, Parisi JE, Perl DP, Peskind E, Petersen RC, Poon WW, Quinn JF, Rajbhandary RA, Raskind M, Reisberg B, Ringman JM, Roberson ED, Rosenberg RN, Sano M, Schneider LS, Seeley W, Shelanski ML, Slifer MA, Smith CD, Sonnen JA, Spina S, Stern RA, Tanzi RE, Trojanowski JQ, Troncoso JC, Van Deerlin VM, Vinters H V., Vonsattel JP, Weintraub S, Welsh-Bohmer KA, Williamson J, Woltjer RL, Cantwell LB, Dombroski BA, Beekly D, Lunetta KL, Martin ER, Kamboh MI, Saykin AJ, Reiman EM, Bennett DA, Morris JC, Montine TJ, Goate AM, Blacker D, Tsuang DW, Hakonarson H, Kukull WA, Foroud TM, Haines JL, Mayeux R, Pericak-Vance MA, Farrer LA, Schellenberg GD (2011) Common variants at MS4A4/MS4A6E, CD2AP, CD33 and EPHA1 are associated with late-onset Alzheimer's disease. *Nat Genet* **43**, 436-441.

[93] De Jager PL, Srivastava G, Lunnon K, Burgess J, Schalkwyk LC, Yu L, Eaton ML, Keenan BT, Ernst J, McCabe C, Tang A, Raj T, Replogle J, Brodeur W, Gabriel S, Chai HS, Younkin C, Younkin SG, Zou F, Szyf M, Epstein CB, Schneider JA, Bernstein BE, Meissner A, Ertekin-Taner N, Chibnik LB, Kellis M, Mill J, Bennett DA (2014) Alzheimer's disease: Early alterations in brain DNA methylation at ANK1, BIN1, RHBDF2 and other loci. *Nat Neurosci* **17**, 1156-1163.

[94] Johnston J, Forsythe ID, Kopp-Scheinpflug C (2010) Going native: Voltage-gated potassium channels controlling neuronal excitability. *J Physiol* **588**(Pt 17), 3187-3200.

[95] Yu SP, Yeh CH, Sensi SL, Gwag BJ, Canzoniero LMT, Farhangrazi ZS, Ying HS, Tian M, Dugan LL, Choi DW (1997) Mediation of neuronal apoptosis by enhancement of outward potassium current. *Science* **278**, 114-117.

[96] Shah NH, Aizenman E (2014) Voltage-gated potassium channels at the crossroads of neuronal function, ischemic tolerance, and neurodegeneration. *Transl Stroke Res* **5**, 38-58.

[97] Choi DW (1996) Ischemia-induced neuronal apoptosis. *Curr Opin Neurobiol* **6**, 667-672.

[98] Thompson CB (1995) Apoptosis in the pathogenesis and treatment of disease. *Science* **267**, 1456-1462.

[99] Su SC, Tsai L-H (2011) Cyclin-dependent kinases in brain development and disease. *Annu Rev Cell Dev Biol* **27**, 465-491.

[100] Chen J, Wang ZF (2010) Roles of cyclin-dependent kinase 5 in central nervous system development and neurodegenerative diseases. *Sheng Li Xue Bao* **62**, 295-308.

[101] Monaco EA, Vallano M Lou (2005) Role of protein kinases in neurodegenerative disease: Cyclin-dependent kinases in Alzheimer's disease. *Front Biosci* **10**, 143-159.

[102] Duhr F, Déléris P, Raynaud F, Séveno M, Morisset-Lopez S, Mannoury La Cour C, Millan MJ, Bockaert J, Marin P, Chaumont-Dubel S (2014) Cdk5 induces constitutive activation of 5-HT 6 receptors to promote neurite growth. *Nat Chem Biol* **10**, 590-597.

[103] Lau LF, Ahlijanian MK (2003) Role of cdk5 in the pathogenesis of Alzheimer's disease. *Neurosignals* **12**, 209-214.

[104] Nishimura YV, Sekine K, Chihama K, Nakajima K, Hoshino M, Nabeshima Y, Kawauchi T (2010) Dissecting the factors involved in the locomotion mode of neuronal migration in the developing cerebral cortex. *J Biol Chem* **285**, 5878-5887.

[105] Carmichael O, Schwarz C, Drucker D, Fletcher E, Harvey D, Beckett L, Jack CR, Weiner M, DeCarli C (2010) Longitudinal changes in white matter disease and cognition in the first year of the Alzheimer disease neuroimaging initiative. *Arch Neurol* **67**, 1370-1378.